

Effects of wall properties and heat transfer on the peristaltic transport of a jeffrey fluid through porous medium channel

Dheia G. Salih Al-Khafajy

College of Computer Science and Mathematics, University of Al-Qadissiya, Diwaniya-Iraq.

E-mail: dr.dheia.g.salih@gmail.com

Ahmed M. Abdulhadi

College of Science, University of Baghdad, Baghdad-Iraq.

E-mail: ahm6161@yahoo.com

Abstract

A mathematical model is constructed to study the effect of heat transfer and elasticity of flexible walls with porous medium in swallowing of food bolus through the oesophagus. The food bolus is supposed to be Jeffrey fluid and the geometry of wall surface of oesophagus is considered as peristaltic wave through porous medium. The expressions for temperature field, axial velocity, transverse velocity and stream function are obtained under the assumptions of low Reynolds number and long wavelength. The effects of thermal conductivity, Grashof number, Darcy number, magnet, rigidity, stiffness of the wall and viscous damping force parameters on velocity, temperature and stream function have been studied. It is noticed that increase in thermal conductivity, Darcy number, Grashof number and the Jeffrey parameter results in increase of velocity distribution. It is found that the size of the trapped bolus increases with increase in the Jeffrey parameter, rigidity and stiffness.

Keywords: Magnetohydrodynamic, Peristaltic transport, Oesophagus, Jeffrey fluid, Porous medium, Food bolus.

1. Introduction

Peristaltic transport is a mechanism of pumping fluids in tubes when progressive wave of area contraction or expansion propagates along the length on the boundary of a distensible tube containing fluid. Peristalsis has quite important applications in many physiological systems and industry. It occurs in swallowing food through the oesophagus, chyme motion in the gastrointestinal tract, in the vasomotion of small blood vessels such as venules, capillaries and arterioles, urine transport from kidney to bladder. In view of these biological and industrial applications, the peristaltic flow has been studied with great interest. Many of the physiological fluids are observed to be non-Newtonian. Peristaltic flow of a single fluid through an infinite tube or channel in the form of sinusoidal wave motion of the tube wall is investigated by Burns and Parkes , Shapiro et al. etc,. In the literature some important analytical studies on peristaltic transport of non–Newtonian fluids are available Devi and Devanathan, Shukla and Gupta, Srivastava and Srivastava, Usha and Rao , Vajravelu et al. (2005a, 2005b),Hayat et al. (2008,2010a,2010b).

Further an interesting fact is that in oesophagus, the movement of food is due to peristalsis. The food moves from mouth to stomach even when upside down. Oesophagus is a long muscular tube commences at the neck opposite the long border of cricoids cartilage and extends from the lower end of the pharynx to the cardiac orifice of the stomach. The swallowing of the food bolus takes place due to the periodic contraction of the esophageal wall. Pressure due to reflexive contraction is exerted on the posterior part of the bolus and the anterior portion experiences relaxation so that the bolus moves ahead. The contraction is practically not symmetric, yet it contracts to zero lumen and squeezes it marvelously without letting any part of the food bolus slip back in the opposite direction. This shows the importance of peristalsis in human beings. Mitra and Prasad studied the influence of wall properties on the Poiseuille flow under peristalsis. Mathematical model for the esophageal swallowing of a food bolus is analyzed by Mishra and Pandey. Kavitha et al. analyzed the peristaltic flow of a micropolar fluid in a vertical channel with longwave length approximation. Reddy et al. studied the effect of thickness of the porous material on the peristaltic pumping when the tube wall is provided with non-erodible porous lining. Lakshminarayana et al. studied the peristaltic pumping of a conducting fluid in a channel with a porous peripheral layer. Radhakrishnamacharya and Srinivasulu studied the influence of wall properties on peristaltic transport with heat transfer. Rathod et al. studied the influence of wall properties on MHD peristaltic transport of dusty fluid. A new model for study the effect of wall properties on peristaltic transport of a viscous fluid has been investigated by Mokhtar and Haroun , Srinivas et al. studied the effect of slip, wall properties and heat transfer on MHD peristaltic transport. Sreenadh et al. studied the effects of wall properties and heat transfer on the peristaltic transport of food bolus through oesophagus. Afsar Khan et al. analyzed the peristaltic transport of a Jeffrey fluid with variable viscosity through a porous medium in an asymmetric channel.

Motivated by this, we consider a mathematical model to study the effect of wall properties and heat transfer on swallowing the food bolus through the oesophagus. The results are analyzed for different values of parameters namely Grashof number, Darcy number, thermal conductivity, magnet, rigidity, stiffness and viscous damping forces of the channel wall through porous medium.

2. Mathematical Formulation

Consider the peristaltic flow of an incompressible Jeffrey fluid in a flexible channel with flexible induced by sinusoidal wave trains propagating with constant speed c along the channel walls.

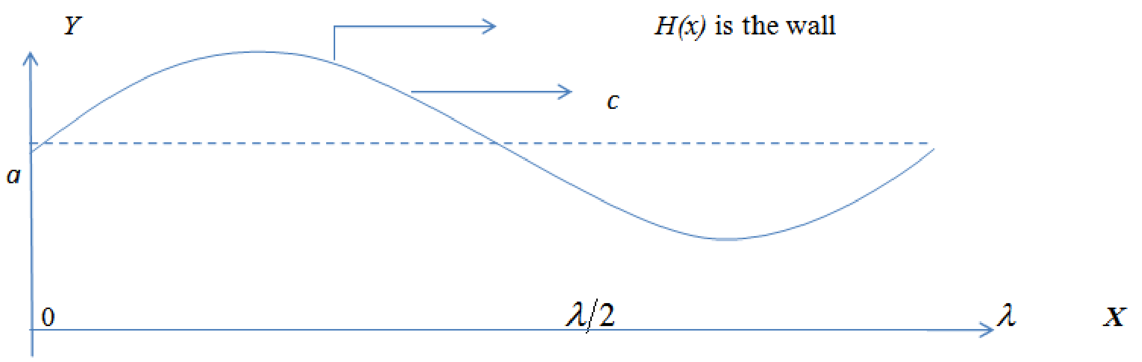

Fig(1) : Geometry of the problem .

The wall deformation is given by

$$H(\bar{x},\bar{t}) = a - \bar{\phi}\cos^2\frac{\pi}{\lambda}(\bar{x} - c\bar{t}) \tag{1}$$

where $\bar{h}$, $\bar{x}$, $\bar{t}$, $\bar{\phi}$, λ and c represent transverse vibration of the wall, axial coordinate, time, half width of the channel, amplitude of the wave, wavelength and wave velocity respectively.

3. Basic equations

The basic equations governing the non-Newtonian incompressible Jeffrey fluid are given by:

The continuity equation is given by:

Mathematical Theory and Modeling
ISSN 2224-5804 (Paper) ISSN 2225-0522 (Online)
Vol.4, No.9, 2014

$$\frac{\partial \bar{u}}{\partial \bar{x}} + \frac{\partial \bar{v}}{\partial \bar{y}} = 0, \tag{2}$$

The momentum equations are:

$$\rho(\frac{\partial \bar{u}}{\partial \bar{t}} + \bar{u}\frac{\partial \bar{u}}{\partial \bar{x}} + \bar{v}\frac{\partial \bar{u}}{\partial \bar{y}}) = -\frac{\partial \bar{p}}{\partial \bar{x}} + \frac{\mu}{1+\lambda_1}(\frac{\partial^2 \bar{u}}{\partial \bar{x}^2} + \frac{\partial^2 \bar{u}}{\partial \bar{y}^2}) + \rho g\alpha(T - T_0) - \sigma B_0^2 \bar{u} - \frac{\mu}{k}\bar{u}, \tag{3}$$

$$\rho(\frac{\partial \bar{v}}{\partial \bar{t}} + \bar{u}\frac{\partial \bar{v}}{\partial \bar{x}} + \bar{v}\frac{\partial \bar{v}}{\partial \bar{y}}) = -\frac{\partial \bar{p}}{\partial \bar{y}} + \frac{\mu}{1+\lambda_1}(\frac{\partial^2 \bar{v}}{\partial \bar{x}^2} + \frac{\partial^2 \bar{v}}{\partial \bar{y}^2}) - \frac{\mu}{k}\bar{v}, \tag{4}$$

The temperature equation is given by:

$$\rho(\frac{\partial T}{\partial \bar{t}} + \bar{u}\frac{\partial T}{\partial \bar{x}} + \bar{v}\frac{\partial T}{\partial \bar{y}}) = \frac{k}{c_p}(\frac{\partial^2 T}{\partial \bar{x}^2} + \frac{\partial^2 T}{\partial \bar{y}^2}) + \Phi, \tag{5}$$

where $\bar{u}$ is the axial velocity, $\bar{u}$ transverse velocity, $\bar{y}$ transverse coordinate, ρ fluid density, $\bar{p}$ pressure, μ fluid viscosity, g acceleration due to gravity, α coefficient of linear thermal expansion of fluid, B_0 magnetic field, T temperature, c_p specific heat at constant pressure, k is the thermal conductivity and Φ constant heat addition/absorption.

The velocity and temperatures at the central line and the wall of the peristaltic channel are given as:
$T = T_0$ at $\bar{y} = 0$
$T = T_1$ at $\bar{y} = \bar{h}$

where T_0 is the temperature at centre is line and T_1 is the temperature on the wall of peristaltic channel.

The governing equation of motion of the flexible wall may be expressed as:

$$L^* = \bar{p} - \bar{p_0} \tag{6}$$

where L^* is an operator, which is used to represent the motion of stretched membrane with viscosity damping forces such that

$$L^* = -\tau\frac{\partial^2}{\partial x^2} + m_1\frac{\partial^2}{\partial t^2} + C\frac{\partial}{\partial t} \tag{7}$$

where τ is the elastic tension in the membrane, m_1 is the mass per unit area, C is the coefficient of viscous damping forces.

Continuity of stress at $y = \bar{h}$ and using momentum equation, yield

$$\frac{\partial}{\partial \bar{x}}L^*(\bar{h}) = \frac{\partial \bar{p}}{\partial \bar{x}} = \frac{\mu}{1+\lambda_1}(\frac{\partial^2 \bar{u}}{\partial \bar{x}^2} + \frac{\partial^2 \bar{u}}{\partial \bar{y}^2}) + \rho g\alpha(T - T_0) - \rho(\frac{\partial \bar{u}}{\partial \bar{t}} + \bar{u}\frac{\partial \bar{u}}{\partial \bar{x}} + \bar{v}\frac{\partial \bar{u}}{\partial \bar{y}}) - \sigma B_0^2 \bar{u} - \frac{\mu}{k}\bar{u} \tag{8}$$

In order to simplify the governing equations of the motion, we may introduce the following dimensionless transformations as follows:

$$\left.\begin{array}{l} x=\dfrac{\bar{x}}{\lambda}, y=\dfrac{\bar{y}}{a}, \delta=\dfrac{a}{\lambda}, u=\dfrac{\bar{u}}{c}, v=\dfrac{\bar{v}}{c\delta}, p=\dfrac{a^2\bar{p}}{\mu\lambda c}, t=\dfrac{c\bar{t}}{\lambda}, \psi=\dfrac{\bar{\psi}}{ac}, Q=\dfrac{\bar{Q}}{as}, \phi=\dfrac{\bar{\phi}}{a}, Da=\dfrac{k}{a^2} \\ \mathrm{Re}=\dfrac{\rho ca}{\mu}, Gr=\dfrac{gpa^2\alpha(T_1-T_0)}{c\mu^2}, \theta=\dfrac{T-T_0}{T_1-T_0}, M^2=\dfrac{\sigma B_0^2 a^2}{\mu}, \beta=\dfrac{a^2\Phi}{k(T_1-T_0)}, \mathrm{Pr}=\dfrac{\mu c_p}{k} \end{array}\right\} \quad (9)$$

where δ is the length of the channel, $\bar{\psi}$ Stream function, $\bar{Q}$ Volume flow rate, Da Darcy number, Re Reynolds number, Gr Grashof number, θ dimensionless temperature, M^2 magnetic parameter, β dimensionless heat source/sink parameter and Pr is Prandtl number.

Substituting (9) into equations (1)-(8), we obtain the following non-dimensional equations and boundary conditions:

$$h(x,t)=1-\phi\cos^2\pi(x-t) \quad (10)$$

$$\frac{\partial u}{\partial x}+\frac{\partial v}{\partial y}=0 \quad (11)$$

$$\mathrm{Re}\,\delta\left(\frac{\partial u}{\partial t}+u\frac{\partial u}{\partial x}+v\frac{\partial u}{\partial y}\right)=-\frac{\partial p}{\partial x}+\frac{1}{1+\lambda_1}\left(\delta^2\frac{\partial^2 u}{\partial x^2}+\frac{\partial^2 u}{\partial y^2}\right)+\frac{\rho g a^2\alpha(T-T_0)}{\mu c}\theta-M^2u-\frac{1}{Da}u \quad (12)$$

$$\mathrm{Re}\,\delta^3\left(\frac{\partial v}{\partial t}+u\frac{\partial v}{\partial x}+v\frac{\partial v}{\partial y}\right)=-\frac{\partial p}{\partial y}+\frac{\delta^2}{1+\lambda_1}\left(\delta^2\frac{\partial^2 v}{\partial x^2}+\frac{\partial^2 v}{\partial y^2}\right)-\frac{\delta^2}{Da}v \quad (13)$$

$$\frac{\mathrm{Re}\,\delta\,\mathrm{Pr}}{(T_1-T_0)}\left(\frac{\partial}{\partial t}+u\frac{\partial}{\partial x}+v\frac{\partial}{\partial y}\right)(\theta(T_1-T_0)+T_0)=\delta^2\frac{\partial^2\theta}{\partial x^2}+\frac{\partial^2\theta}{\partial y^2}+\beta \quad (14)$$

$$\frac{1}{1+\lambda_1}\left(\delta^2\frac{\partial^2 u}{\partial x^2}+\frac{\partial^2 u}{\partial y^2}\right)+Gr\theta-\left(M^2+\frac{1}{Da}\right)u-\mathrm{Re}\,\delta\left(\frac{\partial u}{\partial t}+u\frac{\partial u}{\partial x}+v\frac{\partial u}{\partial y}\right)=\left(E_1\frac{\partial^3 h}{\partial x^3}+E_2\frac{\partial^3 h}{\partial x\partial t^2}+E_3\frac{\partial^2 h}{\partial x\partial t}\right)$$
(15)

$$\left.\begin{array}{ll} \dfrac{\partial u}{\partial y}=0 \text{ at } y=0 & \text{(the regularity condition)} \\ u=0 \text{ at } y=h & \text{(the no slip condition)} \\ v=0 \text{ at } y=0 & \text{(the absence of transverse velocity)} \\ \theta=0 \text{ at } y=0 \text{ and } \theta=1 \text{ at } y=h & \end{array}\right\} \quad (16)$$

4. Solution of the problem

The general solution of the governing equations (10)-(15) in the general case seems to be impossible; therefore, we shall confine the analysis under the assumption of small dimensionless wave number. It follows that $\delta \ll 1$. In other words, we considered the long-wavelength approximation. Along to this assumption, equations (10)-(15) become:

$$h(x,t) = 1 - \phi\cos^2\pi(x-t) \tag{17}$$

$$\frac{\partial u}{\partial x} + \frac{\partial v}{\partial y} = 0 \tag{18}$$

$$\frac{\partial p}{\partial x} = \frac{1}{1+\lambda_1}\frac{\partial^2 u}{\partial y^2} + Gr\theta - (M^2 + \frac{1}{Da})u \tag{19}$$

$$\frac{\partial p}{\partial y} = 0 \tag{20}$$

$$\frac{\partial^2\theta}{\partial y^2} + \beta = 0 \tag{21}$$

$$\frac{1}{1+\lambda_1}\frac{\partial^2 u}{\partial y^2} - (M^2 + \frac{1}{Da})u + Gr\theta = E_1\frac{\partial^2 h}{\partial x^2} + E_2\frac{\partial^2 h}{\partial t^2} + E_3\frac{\partial h}{\partial t} \tag{22}$$

Equation (20) shows that p dependents on x only. The closed form solution for equations (18)-(22) with the boundary conditions Eq. (16) is given by

$$\theta = \frac{y}{h} + \frac{\beta}{2}(hy - y^2) \tag{23}$$

$$\begin{aligned} u = {} & B_1 e^{y\sqrt{(1+\lambda_1)(M^2+\frac{1}{Da})}} + B_2 e^{-y\sqrt{(1+\lambda_1)(M^2+\frac{1}{Da})}} - \frac{Da}{2h(1+\lambda_1)(1+M^2Da)^2}\{4h\beta GrDa + 2h\lambda_1\beta GrM^2Day \\ & + (1+\lambda_1+M^2Da)2h\beta Gry^2 + (1+\lambda_1+\lambda_1M^2+M^2Da)E_3h\pi^2\phi - (1+\lambda_1)(1+M^2Da)[4Gry \\ & + 2h^2\beta Gry + E_3h\pi^2\phi Cos(4\pi(x-t)) + 16E_1h\pi^3\phi Sin(2\pi(x-t)) + 16E_2h\pi^3\phi Sin(2\pi(x-t))]\} \end{aligned} \tag{24}$$

where B_1 and B_2 are constants can be determinates by using the boundary conditions Eq. (16).

The corresponding Stream function ($u = \frac{\partial\psi}{\partial y}$) can be obtained by integrating Eq. (24) and using the condition $\psi = 0$ at $y = 0$. It is given by

$$\begin{aligned} \psi = {} & -\frac{\beta GrM^2Day^3}{3+3M^2Da} + \frac{(2+h^2\beta)GrDay^2}{2h(1+M^2Da)} - \frac{B_2e^{-y\sqrt{(1+\lambda_1)(M^2+\frac{1}{Da})}}}{\sqrt{(1+\lambda_1)(M^2+\frac{1}{Da})}} + \frac{B_1e^{y\sqrt{(1+\lambda_1)(M^2+\frac{1}{Da})}}}{\sqrt{(1+\lambda_1)(M^2+\frac{1}{Da})}} \\ & - \frac{1}{2(1+\lambda_1)(1+M^2Da)^2}Day(4\beta GrDa + (1+\lambda_1)(1+M^2Da)E_3\pi^2\phi \\ & - E_3(1+\lambda_1)(1+M^2Da)\pi^2\phi Cos(4\pi(x-t)) \\ & - 16(E_1+E_2)(1+\lambda_1)(1+M^2Da)\pi^2\phi Sin(2\pi(x-t))) + \frac{B_1 - B_2}{\sqrt{(1+\lambda_1)(M^2+\frac{1}{Da})}} \end{aligned} \tag{25}$$

5. Results and Discussion

In this section, the numerical and computational results are discussed for the problem of an incompressible non-Newtonian Jeffrey fluid in the channel with heat and mass transfer through the graphical illustrations. The numerical evaluations of the analytical results and some important results are displayed graphically in Figure (2)-(20). MATHEMATICA program is used to find out numerical results and illustrations.

From Figure (2) displays the effect of rigidity parameter in the presence of stiffness $(E_2 \neq 0)$ and viscous damping force $(E_3 \neq 0)$. It is noticed that the velocity increases with increase in rigidity parameter. A similar observation is made for different values of E_2 in the presence of other parameters i.e., rigidity and viscous damping force which is shown in Figure (3).

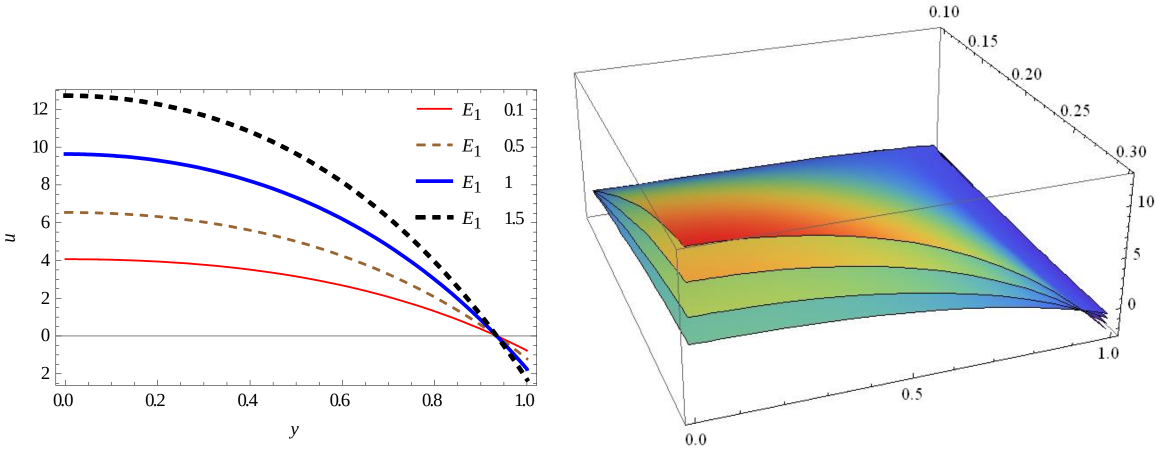

Fig 2. Velocity distribution for different values of E_1 with
$x = 0.5, t = 0.1, E_2 = 0.5, E_3 = 0.5, Gr = 2, \lambda_1 = 0.2, \phi = 0.1, \beta = 2, Da = 0.7, M = 0.9.$

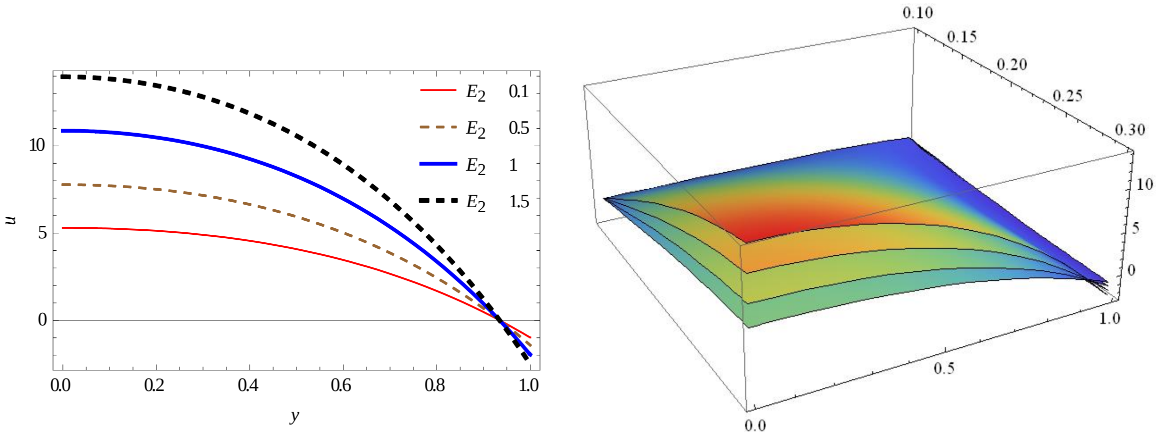

Fig 3. Velocity distribution for different values of E_2 with
$x = 0.3, t = 0.1, E_1 = 0.7, E_3 = 0.5, Gr = 2, \lambda_1 = 0.2, \phi = 0.1, \beta = 2, Da = 0.7, M = 0.9.$

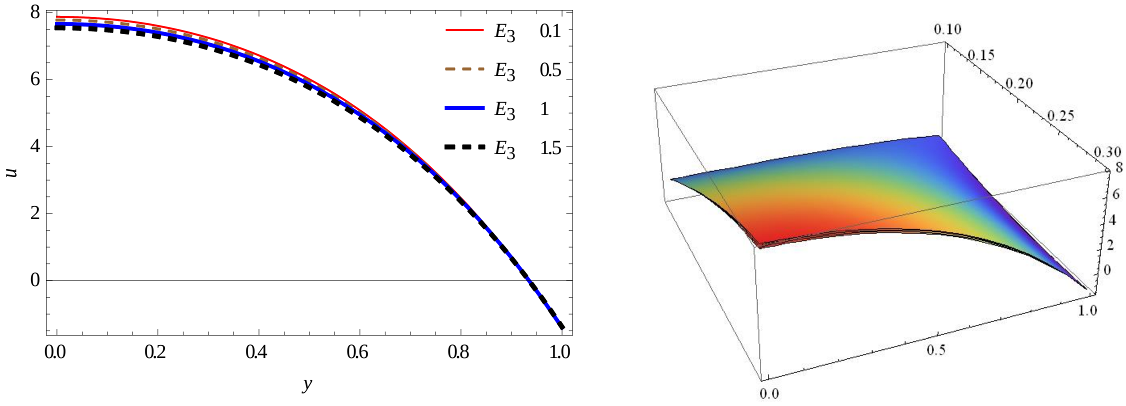

Fig 4. Velocity distribution for different values of E_3 with

$x=0.3, t=0.1, E_1=0.7, E_2=0.5, Gr=2, \lambda_1=0.2, \phi=0.1, \beta=2, Da=0.7, M=0.9$.

From figure (4), we can see the influence of viscous damping force on velocity distribution in the presence of rigidity and stiffness. One can observe that the velocity decreases with the increase in E_3. Figure(5), illustrates the effect of the parameter Grashof number *Gr* on velocity distribution we see that *u* increases with the increasing of *Gr* when $y < 1$. Figures (6) and (7), it is observed that increase in Jeffrey parameter λ_1 and thermal conductivity β results in increase of velocity distribution

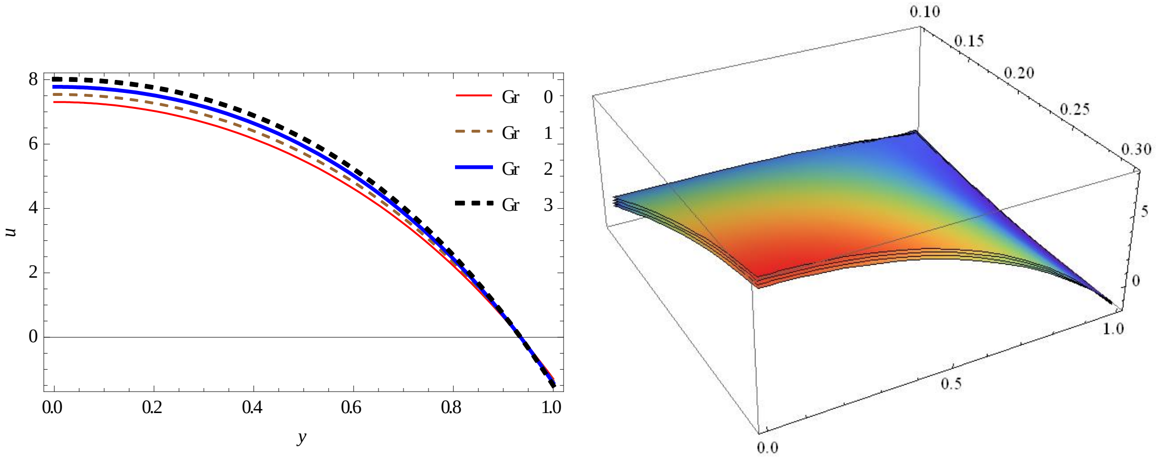

Fig 5. Velocity distribution for different values of *Gr* with

$x=0.3, t=0.1, E_1=0.7, E_3=0.5, E_3=0.5, \lambda_1=0.2, \phi=0.1, \beta=2, Da=0.7, M=0.9$.

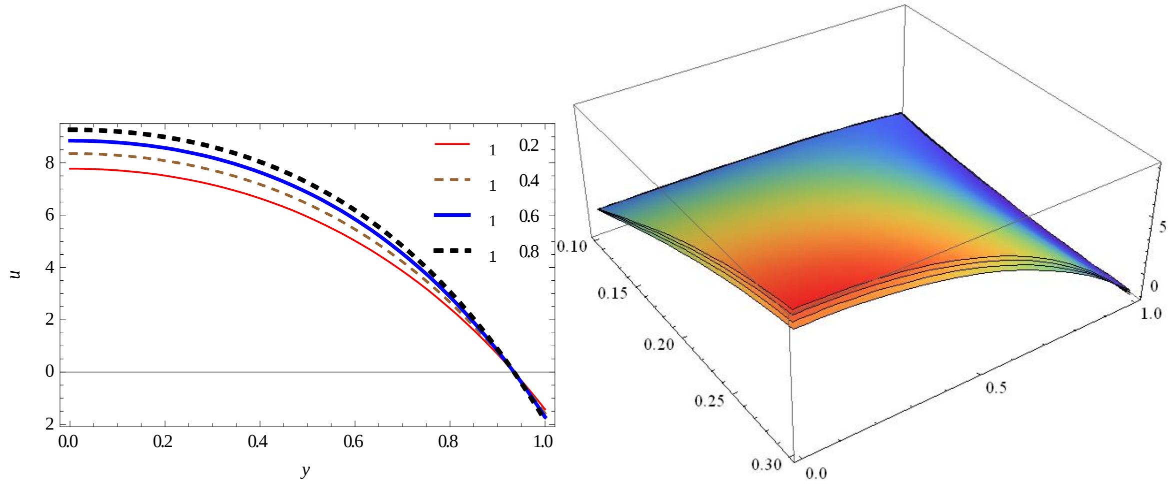

Fig 6. Velocity distribution for different values of λ_1 **with**

$x = 0.3, t = 0.1, E_1 = 0.7, E_3 = 0.5, E_3 = 0.5, Gr = 2, \phi = 0.1, \beta = 2, Da = 0.7, M = 0.9$.

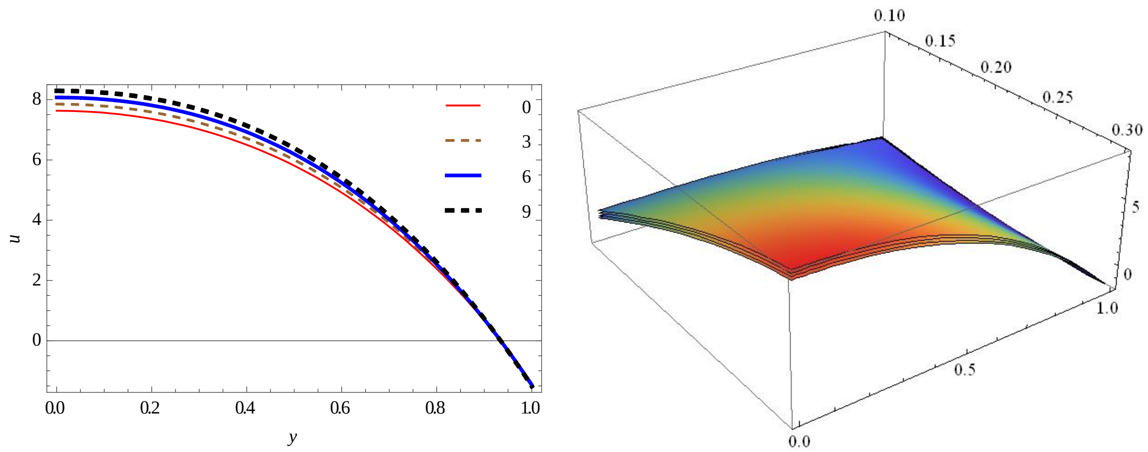

Fig 7. Velocity distribution for different values of β **with**

$x = 0.3, t = 0.1, E_1 = 0.7, E_3 = 0.5, E_3 = 0.5, Gr = 2, \phi = 0.1, \lambda_1 = 0.2, Da = 0.7, M = 0.9$.

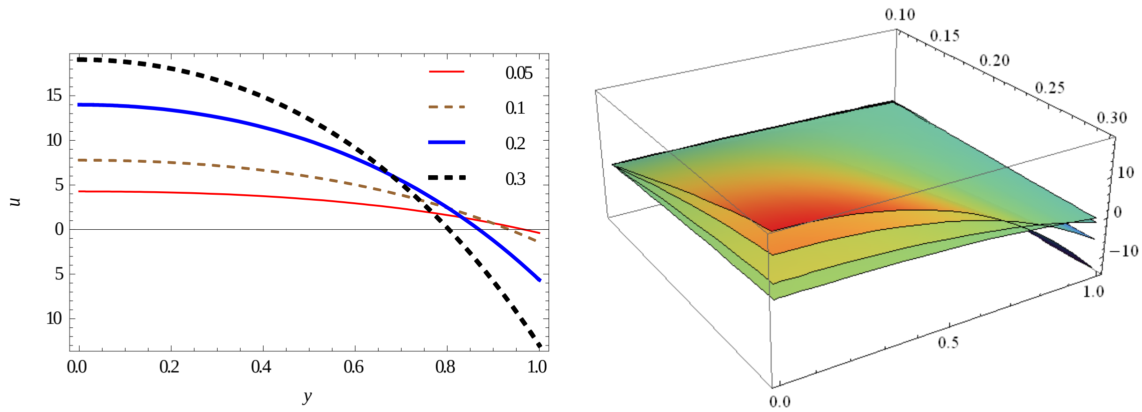

Fig 8. Velocity distribution for different values of ϕ **with**

$x = 0.3, t = 0.1, E_1 = 0.7, E_3 = 0.5, E_3 = 0.5, Gr = 2, M = 0.9, \lambda_1 = 0.2, Da = 0.7, \beta = 2$.

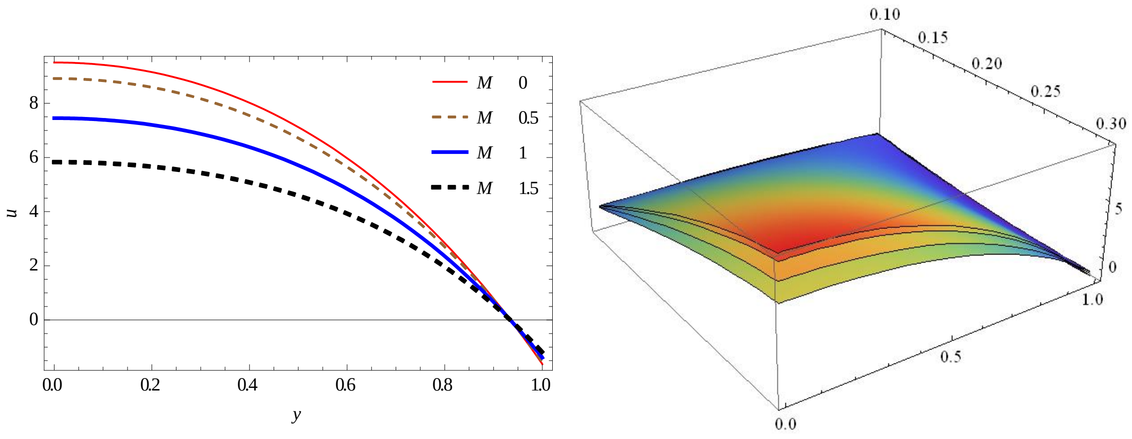

Fig 9. Velocity distribution for different values of M with

$x=0.3, t=0.1, E_1=0.7, E_3=0.5, E_3=0.5, Gr=2, \phi=0.1, \lambda_1=0.2, Da=0.7, \beta=2$.

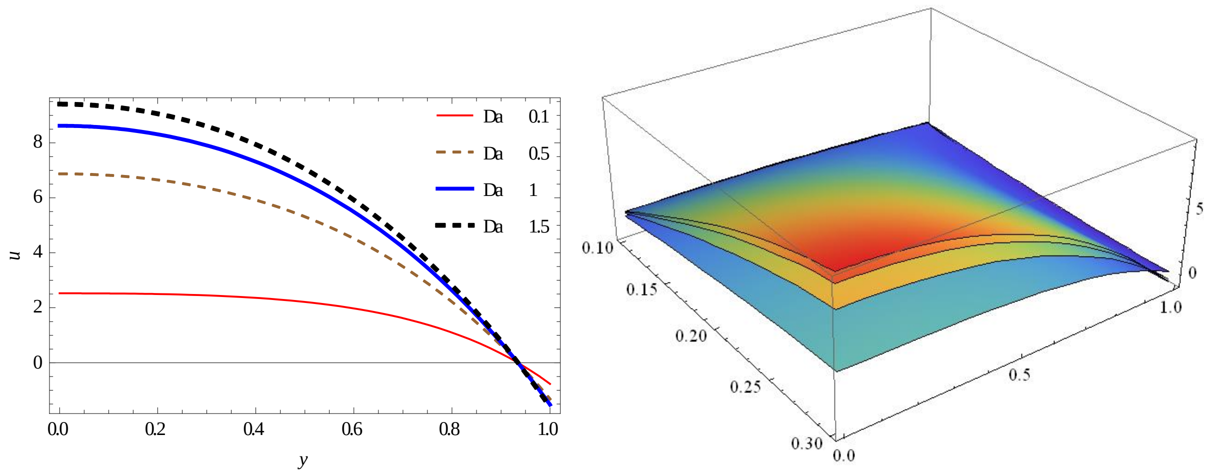

Fig 10. Velocity distribution for different values of *Da* with

$x=0.3, t=0.1, E_1=0.7, E_3=0.5, E_3=0.5, \lambda_1=0.2, Gr=2, \beta=2, \phi=0.1, M=0.9$.

Figure (8) show that velocity distribution increases with the increasing of ϕ. Figure (9) show that velocity distribution decreases with the increasing of magnetic parameter M, while Figure (10) it is observed that increase in Darcy number Da results in increase of velocity distribution. The variation in temperature for various values of thermal conductivity is shown in Figure (11). The temperature increases with the increase in β.The variation in temperature for various values of thermal conductivity is shown in Figure (10). The temperature increases with the increase in β.

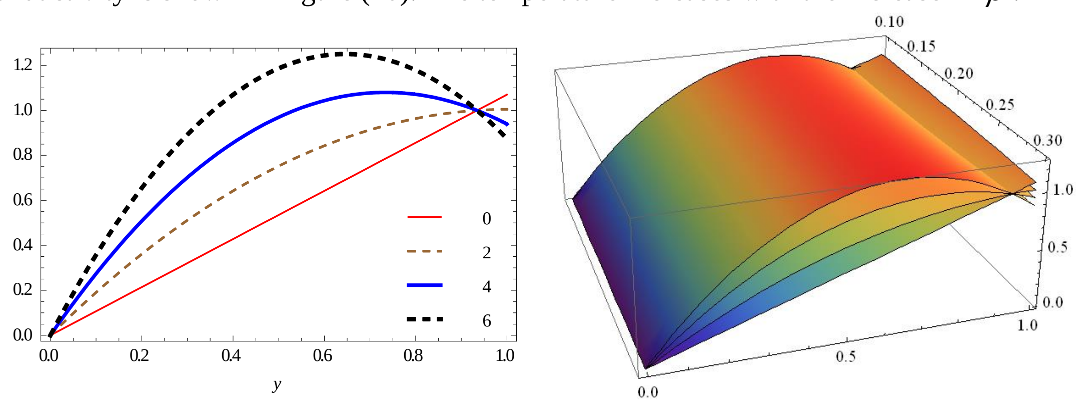

Fig 11. Velocity distribution for different values of β with $x=0.3, t=0.1, \phi=0.1$.

www.iiste.org

6. Trapping phenomenon

The formation of an internally circulating bolus of fluid by closed streamlines is called trapping and this trapped bolus is pushed ahead along with the peristaltic wave. The effects of E_1, E_2, E_3, β, *Gr*, λ_1, M and D_a on trapping can be seen through Figures (12)-(20). Fig.(12) show that the size of the trapped bolus increase with the increase in E_1. Fig.(13) is plotted, the effect of E_2 on trapping, the size of the trapped bolus increase with the increase in E_2. Fig.(14) show that the size of the trapped bolus decrease with the increase in E_3. The effect of thermal conductivity on trapping is analyzed in Figure (15). It can be concluded that the size of the trapped bolus in the left side of the channel decreases when β increases where as it has opposite behavior in the right hand side of the channel. The influence of Grashof number *Gr* on trapping is analyzed in Figure (16). It shows that the size of the left trapped bolus decreases with increase in *Gr* where as the size of the right trapped bolus increases with increase in *Gr*. The effect of λ_1 on trapping can be seen in Figure (17). We notice that the size of the bolus increases with increase λ_1. The effect of ϕ on trapping is analyzed in Figure (18). We notice that the size of the bolus increases with increase ϕ.

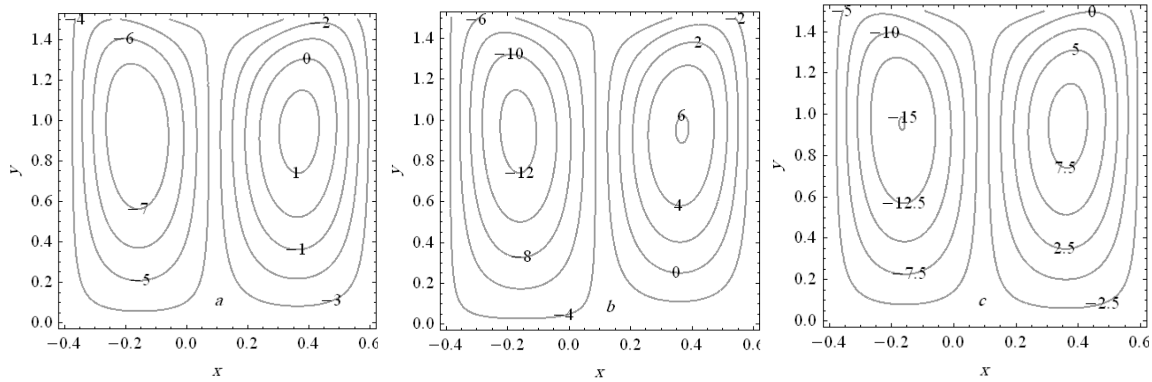

Fig.12 Graph of the streamlines for four different values of E_1; (a) E_1 = 0.5, (b) E_1 = 1.5, and (c) E_1 = 2 at

$t = 0.1, E_2 = 0.5, E_3 = 0.5, Da = 0.9, M = 0.9, Gr = 2, \lambda_1 = 0.2, \phi = 0.1, \beta = 2$.

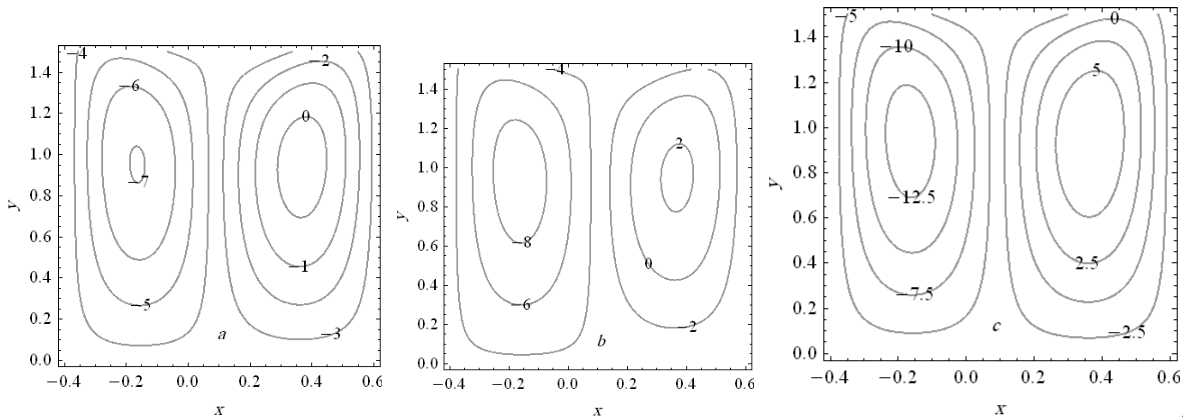

Fi

g.13 Graph of the streamlines for four different values of E_2; (a) E_2 = 0.1, (b) E_2 = 0.5, and (c) E_2 = 1.5 at

$t = 0.1, E_1 = 0.7, E_3 = 0.5, Da = 0.9, M = 0.9, Gr = 2, \lambda_1 = 0.2, \phi = 0.1, \beta = 2$.

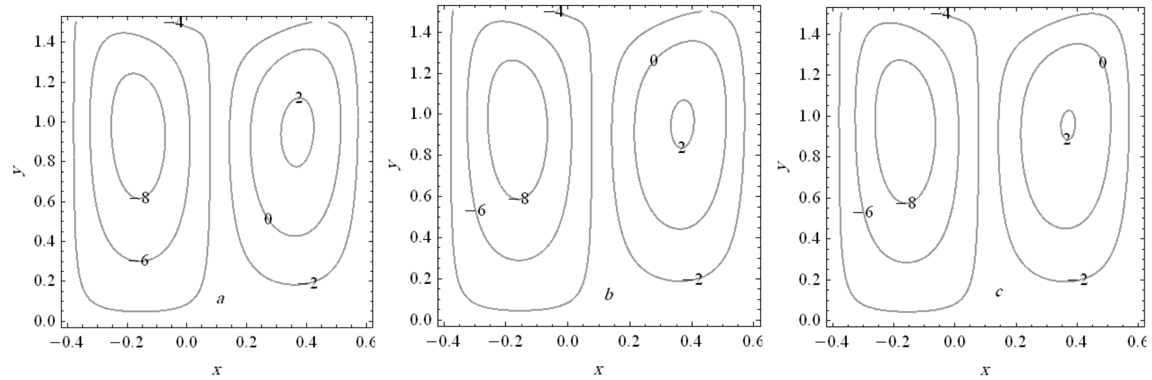

Fig.14 Graph of the streamlines for four different values of E_3; (a) E_3 = 0.5, (b) E_3 = 1.5, and (c) E_3 = 2 at

$$t = 0.1, E_1 = 0.7, E_2 = 0.5, Da = 0.9, M = 0.9, Gr = 2, \lambda_1 = 0.2, \phi = 0.1, \beta = 2.$$

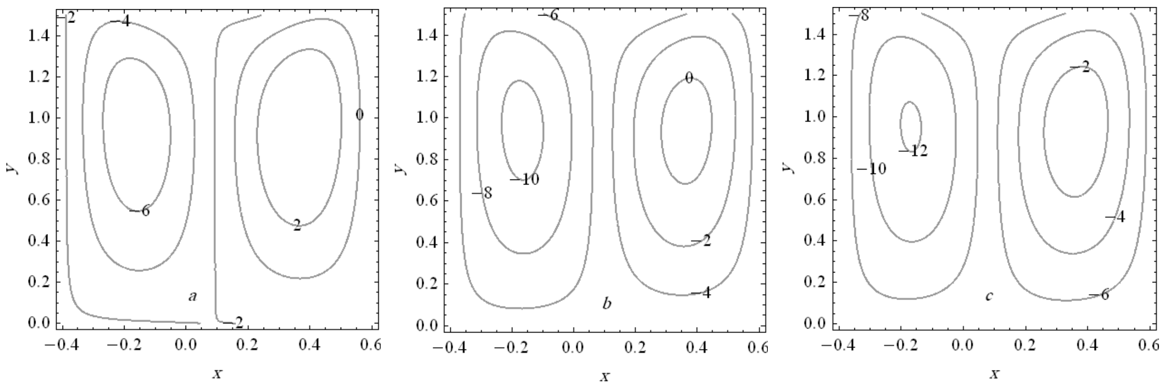

Fig. 15 Graph of the streamlines for four different values of β; (a) β = 0, (b) β = 4, and (c) β = 6 at

$$t = 0.1, E_1 = 0.7, E_3 = 0.5, E_3 = 0.5, Da = 0.9, M = 0.9, Gr = 2, \phi = 0.1, \lambda_1 = 0.2.$$

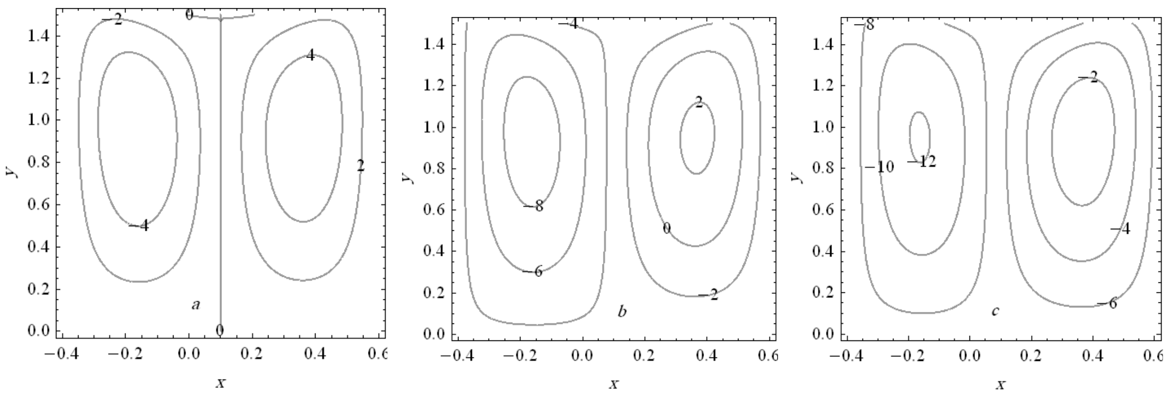

Fig.16 Graph of the streamlines for four different values of *Gr*; (a) *Gr* = 0, (b) *Gr* = 2, and (c) *Gr* = 4

at $t = 0.1, E_1 = 0.7, E_3 = 0.5, E_3 = 0.5, Da = 0.9, M = 0.9, \lambda_1 = 0.2, \phi = 0.1, \beta = 2.$

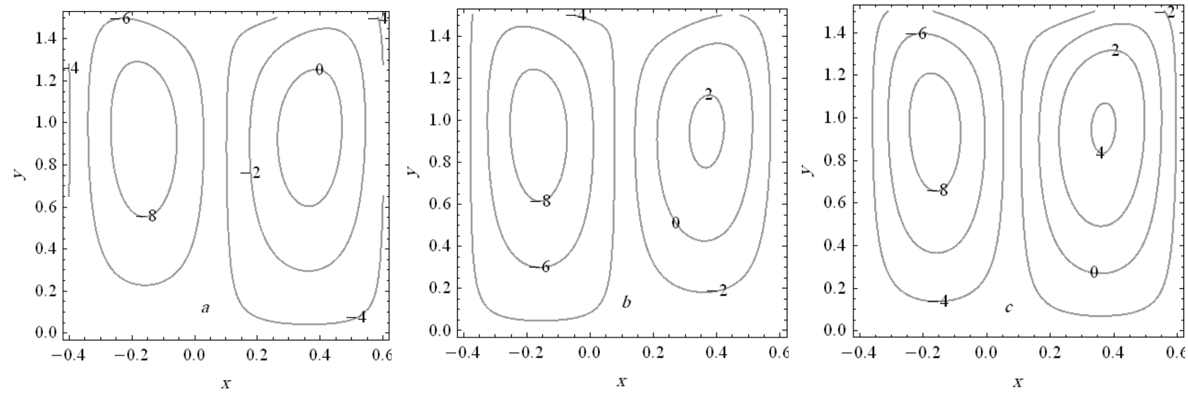

Fig.17 Graph of the streamlines for four different values of λ_1; (a) λ_1 = 0, (b) λ_1 = 0.2, and (c) λ_1 = 0.6 at

$t=0.1, E_1=0.7, E_3=0.5, E_3=0.5, Da=0.9, M=0.9, Gr=2, \phi=0.1, \beta=2$.

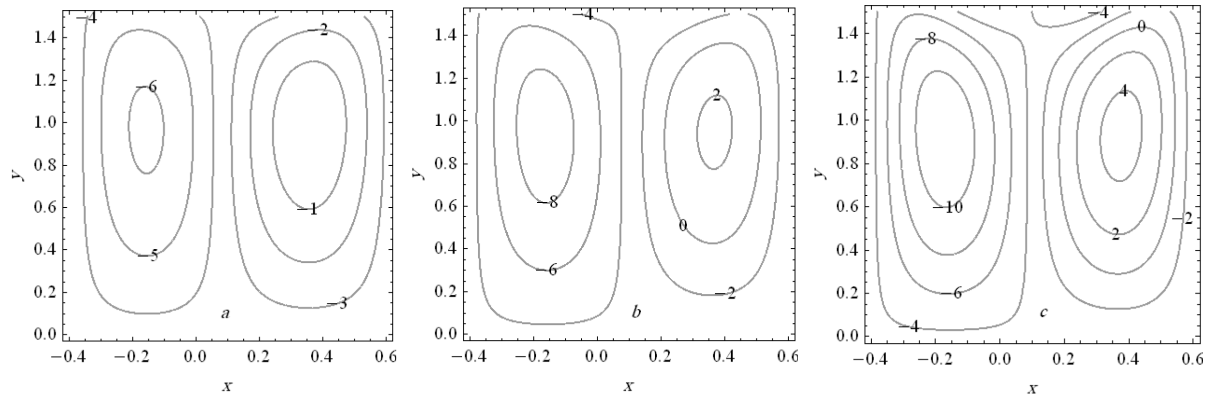

Fig.18 Graph of the streamlines for four different values of ϕ; (a) ϕ = 0.05, (b) ϕ = 0.1, and (c) ϕ = 0.15 at

$t=0.1, E_1=0.7, E_3=0.5, E_3=0.5, Da=0.9, M=0.9, Gr=2, \lambda_1=0.2, \beta=2$.

The influence of Darcy number *Da* on trapping is analyzed in Figure (19). It shows that the size of the left trapped bolus decreases with increase in *Da* where as the size of the right trapped bolus increases with increase in *Da*. And Figure (20) show that influence of *M* on trapping. It shows that the size of the left trapped bolus increases with increase in *M* where as the size of the right trapped bolus decreases with increase in *M*.

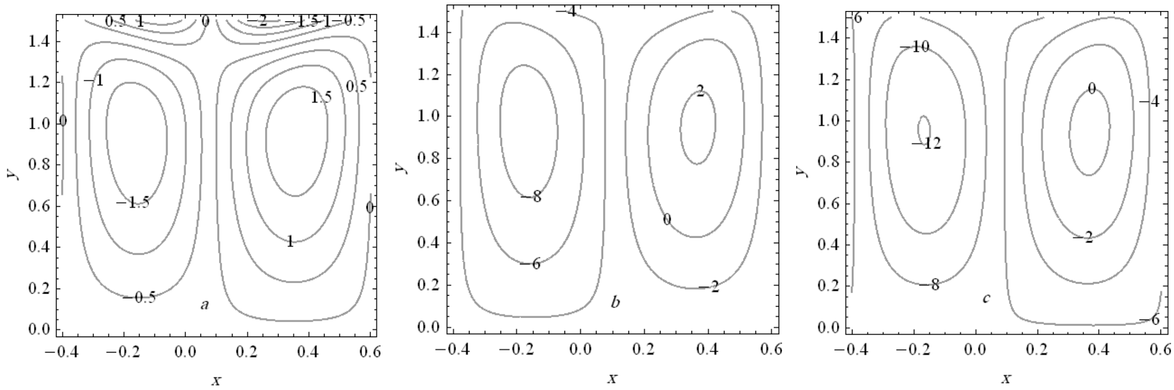

Fig.19 Graph of the streamlines for four different values of *Da*; (a) *Da* = 0.1, (b) *Da* = 0.9, and (c) *Da* = 1.5 at

$t=0.1, E_1=0.7, E_3=0.5, E_3=0.5, M=0.9, Gr=2, \lambda_1=0.2, \phi=0.1, \beta=2.$

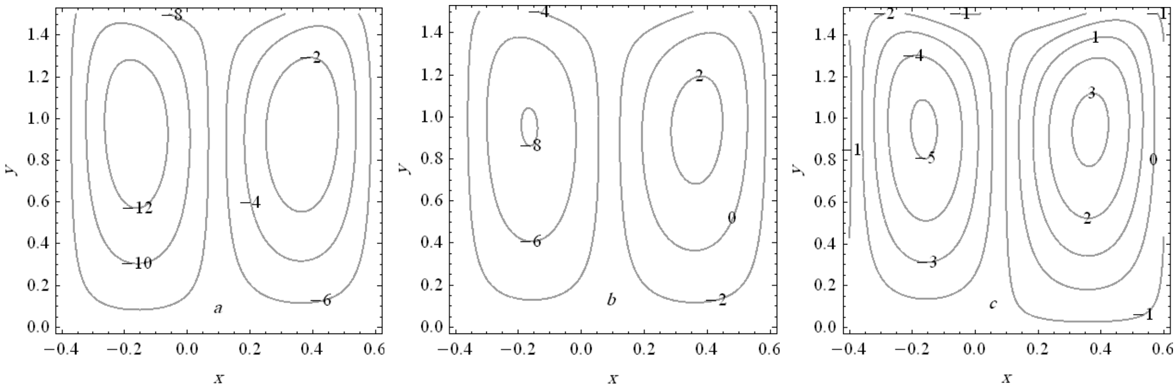

Fig.20 Graph of the streamlines for four different values of *M*; (a) *M* = 0.5, (b) *M* = 1, and (c) *M* = 1.5 at

$t=0.1, E_1=0.7, E_3=0.5, E_3=0.5, Da=0.9, Gr=2, \lambda_1=0.2, \phi=0.1, \beta=2.$

7- Concluding remarks

The present study deals with the combined effect of wall properties and heat transfer on the peristaltic transport of a Jeffrey fluid through porous medium channel. We obtained the analytical solution of the problem under long wavelength and low Reynolds number assumptions. The results are analyzed for different values of pertinent parameters namely Grashof number, Darcy number, thermal conductivity, rigidity, stiffness, magnet and viscous damping forces of the channel wall. Some of the interesting findings are;

1. The axial velocity increases with the increase in E_1, E_2, β, *Gr*, *Da*, ϕ and λ_1. Further, the axial velocity decreases with increase in E_3 and *M*. and attains its maximum height at y = 0, as specified by the boundary conditions.

2. The volume of the trapped bolus increases with increase in E_1, E_2 and ϕ. Moreover, more trapped bolus appears with increase in E_1, E_2 and ϕ.

3. The volume of the trapped bolus decreases with increase in E_3.

4. The volume of the left trapped bolus decreases with increase in β, *Gr*, *Da*, where as it has opposite behavior in the right hand side of the channel. And inversion with respect to λ_1 and *M*.

5. The coefficient of temperature increases with increasing values of thermal conductivity.

REFERENCES

Burns JC and Parkes T, **1967**, *Journal of Fluid Mechanics*, 29, 731-734.

Shapiro AH, Jaffrin MY and Weinberg SL, **1969**, *Journal of Fluid Mechanics*, 37, 799-825.
Devi G and Devanathan R, **1975**, *Proceedings of Indian Academy Science*, 81A, 149-163.
Shukla JB and Gupta SP, **1982**, *Journal of Biomechanical Engineering*, 104, 182-186.
Srivastava LM and Srivastava VP, **1984**, *Journal of Biomechanics*, 17, 821-829.
Usha S and Rao AR, **1995**, *Journal of Biomechanics*, 28, 45-52.
Vajravelu K, Sreenadh S and Ramesh Babu V, **2005a**, *International Journal of Nonlinear Mechanics*, 40, 83-90.
Vajravelu K, Sreenadh S and Ramesh Babu V, **2005b**, *Applied Mathematics and Computation*, 169, 726-735.
Hayat T and Ali N, **2008**, *Communication in Nonlinear Science and Numerical Simulation*, 12, 1343-1352.
Hayat W, Sallem N and Ali N, **2010a**, *Communication in Nonlinear Science and Numerical Simulation*, 15, 2407-2423.
Hayat T, Sajjad R and Asghar S, **2010b**, *Communication in Nonlinear science and Numerical simulation*, 15, 2400-2406.
Mitra T K and Prasad S N, **1973**, *Journal of Biomechanics*, 6, 681-693.
Mishra JC and Pandey SK, **2001**, *Mathematical and computer modelling*, 33,997-1009.
Kavitha A, Hemadri Reddy R, Sreenadh S, Saravana R and Srinivas ANS, **2011**, *Advances in applied Science Research*, 2(1), 269-279.
Hemadri Reddy R, Kavitha A, Sreenadh S, and Hariprabhakaran P, **2011**, *Advances in applied Science Research*, 2(2), 167-178.
Lakshminarayana P, Sreenadh S and Sucharitha G, **2012**, *Advances in Applied Science Research*, 3(5), 2890-2899.
Radhakrishnamacharya G and Srinivasulu Ch, **2007**, *Computer Rendus Mecanique*, 335, 369-373.
Rathod VP and Pallavi Kulkarni, **2011**, *Advances in applied Science Research*, 2(3), 265-279.
Mokhtar A Abd Elnaby and Haroun MH, **2008**, Communication in Nonlinear Science and Numerical simulation, 13, 752-762.
Srinivas S, Gayathri R and Kothandapani M, **2009**, *Computer Physics Communications*, 180, 2116-2112.
Sreenadh S, Uma Shankar C and Raga Pallavi A, **2012**, *Int.J.of Appl.Math and Mech*, 8(7), 93-108.
Afsar khan A, Ellahi R, and Vafai.K., **2012**, *Advances in Mathematical Physics*, 1-15.